Hydrol. Earth Syst. Sci. Discuss., 7, 417–440, 2010
www.hydrol-earth-syst-sci-discuss.net/7/417/2010/

Hydrology and Earth System Sciences Discussions

This discussion paper is/has been under review for the journal Hydrology and Earth System Sciences (HESS). Please refer to the corresponding final paper in HESS if available.

Assessing the application of a laser rangefinder for determining snow depth in inaccessible alpine terrain

J. L. Hood and M. Hayashi

Geoscience, University of Calgary, 2500 University Dr. NW, Calgary, AB T2N 1N4, Canada

Received: 11 December 2009 – Accepted: 23 December 2009 – Published: 19 January 2010

Correspondence to: J. L. Hood (jlhood@ucalgary.ca)

Published by Copernicus Publications on behalf of the European Geosciences Union.

Abstract

Snow is a major contributor to stream flow in alpine watersheds and quantifying snow depth and distribution is important for hydrological research. However, direct measurement of snow in rugged alpine terrain is often impossible due to avalanche and rock fall hazard. A laser rangefinder was used to determine the depth of snow in inaccessible areas. Laser rangefinders use ground based light detection and ranging technology but are more cost effective than airborne surveys or terrestrial laser scanning systems and are highly portable. Data was collected within the Opabin watershed in the Canadian Rockies. Surveys were conducted on one accessible slope for validation purposes and two inaccessible talus slopes. Laser distance data was used to generate surface models of slopes when snow covered and snow-free and snow depth distribution was quantified by differencing the two surfaces. The results were compared with manually probed snow depths on the accessible slope. The accuracy of the laser rangefinder method as compared to probed depths was 0.21 m or 12% of average snow depth. Results from the two inaccessible talus slopes showed regions near the top of the slopes with 6–9 m of snow accumulation. These deep snow accumulation zones result from re-distribution of snow by avalanches and are hydrologically significant as they persist until late summer.

1 Introduction

Snow is a major component of the annual water balance in alpine watersheds, and snow depth and distribution measurements are important to hydrological research. However, direct measurement of snow is time consuming, and in many alpine areas, often impractical or impossible due to steep slopes with rock fall and avalanche hazard. In high elevation mountain regions, snowmelt influences the timing and quantity of water delivered to rivers and streams. Hydrological process studies in alpine headwaters are important to understand what changes may occur within a changed climatic

HESSD

7, 417–440, 2010

Assessing the application of a laser rangefinder

J. L. Hood and M. Hayashi

regime. There are already indications that snow melt is occurring earlier in the year (Barnett et al., 2005) and that the elevation at which precipitation transitions from rain to snow is rising (Hamlet et al., 2005). Accurately quantifying snow depth and distribution is also important for operational stream flow forecasting, validation of climate and hydrological models and applications in avalanche forecasting and research.

Manual measurement of snow depth and density is routinely carried out in both operational settings and in field research studies. Manual measurement involves collecting snow depth and density measurements at discrete points (Elder et al., 1991) which must be interpolated to gain insight into how snow is continuously distributed. Manual snow surveys are time and labour intensive, and extensive snow surveys are not practical outside of research studies in small watersheds. Additionally, in alpine watersheds, avalanche and rock fall hazard limits which areas can be surveyed safely. As a result of the above limitations, extensive resources have been directed towards remote methods of determining snow pack properties such as snow covered area (SCA), snow depth, density and snow water equivalent (SWE). A method that is able to determine all of these properties simultaneously does not yet exist. Satellite imagery can be useful in delineating SCA at high spatial and temporal resolution (Dozier and Painter, 2004; Rosenthal and Dozier, 1996). It is, however, limited by difficulties in data capture due to frequently cloudy conditions in mountain regions and does not provide information regarding snow volume. The acquisition of light detection and ranging (LiDAR) data can be used to determine snow depth (Hopkinson et al., 2001) when a snow covered dataset and a snow-free dataset are differenced. LiDAR data has recently been used for investigating spatial snow distribution in Colorado (Trujillo et al., 2007, 2009; Fassnacht and Deems, 2006; Deems et al., 2006) although, at present, acquisition of LiDAR data is very expensive and requires special expertise. Passive microwave sensors mounted on satellites show promise for determining snow water equivalence (SWE) and these methods continue to improve (Foster et al., 2005); however, the spatial resolution remains too coarse for studies in small watersheds and is limited by underestimation of SWE in alpine regions (Foster et al., 2005).

Terrestrial laser scanning (TLS) is a ground-based LiDAR technique that is capable of producing high spatial resolution scans of the surface and has been used in numerous applications including determining snow depth in alpine terrain for use in avalanche research (Prokop, 2008; Prokop et al., 2008, Schaffhauser et al., 2008). Prokop (2008) and Prokop et. al. (2008) were able to measure snow depth to within 10 cm. However, TLS units are at present quite expensive and outside of the domain of many research budgets. Laser rangefinder distance devices are based on the same laser technology as TLS, but rely on manual point data retrieval instead of scanning. Laser rangefinders can be purchased for a fraction of the price of TLS units and for small scale applications they present a viable alternative for determining distances to inaccessible areas. Laser rangefinders have been used previously in diverse research applications such as structural bedrock mapping of the Sheep Mountain anticline (Allwardt et al., 2007), mapping of ground fissures involved in coal bed fires (Ide et al., 2009) and recording positions of rutting elk and their behaviour with regards to vehicle traffic (St. Clair and Forrest, 2009). A laser rangefinder has also been used to create small scale digital terrain models by interpolating point measurements (Lewicki et al., 2007). To our knowledge, use of a laser rangefinder for determining distributed snow depth is a unique application of this technique. The laser model used in this study was a Lasercraft Contour XLRic which can be purchased for a modest price. Additionally, this system has the advantage of being very portable with all of the necessary equipment easily transported by a single person. Therefore, a laser rangefinder is a potentially viable alternative to TLS for measuring snow depth.

In this study we attempt to use a laser rangefinder distance device to assess the depth of snow in dangerous to access areas within the Opabin watershed in the Canadian Rockies (see site description below). Approximately 58% of the watershed is inaccessible because of extremely rugged terrain. Slope angles in the inaccessible region are dominantly greater than 50 degrees and accumulated snow is transported to lower elevations via spindrift and small slough avalanches. The snow in these preferential accumulation zones is an important component of the annual snowpack and often persists through to the end of the summer months. These zones comprise 8% of the watershed but are typically inaccessible for manual snow measurements due to exposure to rock fall and avalanche hazard. Therefore, the objectives of this study were to: (1) assess the applicability of a laser distance device for determining maximum snow accumulation and (2) assess the hydrological significance of increased snow accumulation at the base of steep cliff walls from spindrift and slough avalanching.

2 Methods

2.1 Laser specifications

A bi-pod mounted laser rangefinder (Lasercraft Contour XLRic) (Table 1) was used to generate a dataset of surface elevations of snow-covered surfaces. The laser rangefinder is based on LiDAR technology where an infrared laser signal is transmitted and returned from a surface. The time delay between transmission and receipt of the signal is used to determine the distance to the target based on the speed of light (Lasercraft, 2007). In addition to distance, point data collected with the laser provides measurement offsets from the laser position which include inclination and azimuth. If the precise location of the laser is known, the horizontal coordinates and elevation can be determined using simple geometric calculations. The point elevation data is then interpolated to generate a digital elevation surface and surfaces generated from subsequent surveys are differenced to obtain the change in elevation. The laser wavelength is 905 nm (Table 1) and has excellent signal return from white surfaces such as snow. The Contour XLRic has a maximum range of 1850 m which allows for surveying from safe locations. However, positional uncertainty becomes an issue at large distances as the inclination accuracy (±0.1 degree) and the bearing accuracy (±0.5 degree) results in accuracy of approximately 4.3 m at a shooting range of 500 m. Additionally, an increase in the size of the beam with distance also limits the accuracy at full range. A maximum range of 500 m was used in this study. A common concern with laser sur-

HESSD

7, 417–440, 2010

Assessing the application of a laser rangefinder

J. L. Hood and M. Hayashi

veying is transmission of the beam into the snow surface. A study using TLS (laser wavelength of 900 nm) found that transmission into snow as compared to a snow surface covered by a foil blanket was negligible (Prokop, 2008).

The laser rangefinder has similarities and differences from a TLS system that make it both more and less suitable for this application. Both methods involve creating a digital elevation surface by interpolating point measurements; however, the TLS method generates a higher resolution dataset (Prokop, 2008) which enables smaller features to be resolved. In contrast, interpolating lower spatial resolution point data from a laser rangefinder (Table 2) results in a more generalized surface and introduces greater uncertainty from the interpolation method. TLS models typically have a smaller beam divergence than a laser rangefinder (Table 1) which further aids in resolution of small scale features. Both systems require adequate signal return to determine the distance to the surface and are impacted by conditions such as fog and lower signal return from wet snow surfaces (Prokop, 2008). Although high spatial resolution is generally a desirable result, for the purpose of the present study, determining snow depth in deep accumulation areas (2–10 m) does not necessitate a vertical resolution of centimetres. The objective measure of satisfactory results for this study is an uncertainty of 10–15% of average snow depth.

2.2 Study site

This research was conducted in the Opabin watershed within the Lake O'Hara Research Basin (51.35° N, 116.32° E) (Fig. 1). This area is a headwaters alpine watershed located within Yoho National Park, British Columbia along the western side of the continental divide. The topography is extremely rugged, with elevations ranging from 2000–3400 m. Slope angles range from 0–87° with a mean watershed slope of 33°. In the interior of the watershed, the Opabin "plateau" has slope angles of less than 35° whereas the surrounding cirque walls are dominantly greater than 50° with many zones of near vertical cliff walls. An automatic weather station (Fig. 1) was installed in August 2004 to measure temperature, humidity, wind speed and direction, precipitation, snow depth, and radiation. The watershed has an annual average precipitation of 1000–1200 mm, average snow pack of 575–700 mm water equivalent and is snow-covered from November through to June or July. The geology of the watershed consists of quartzite and sandstone at lower elevations (valley bottom) with dominantly carbonates at upper elevations (mountain peaks) (Lickorish and Simony, 1995).

The steep cirque walls results in transport of snow from higher elevations to lower elevations through the continual process of spindrift and slough avalanches. The cirque walls are too steep to accumulate significant amounts of snow therefore mass movement of snow (i.e. large point release or slab avalanches) only occurs in a few localized areas. The cliff walls are also prone to significant rock fall as a result of the friable carbonate geology at upper elevations and multiple small fault zones. The combination of snow transport and rock fall potential makes it extremely hazardous to deploy field teams for manual measurement of snow depth and density in a portion of the watershed; however, these areas are zones of preferential accumulation.

Two areas ("upper talus" slope and "lower talus" slope) were targeted for this analysis in order to quantify snow accumulation at the base of cliff walls. In a third location ("validation slope") both laser data and manually measured snow depth data were collected for the purpose of validating laser results. The validation slope is located in the interior of the watershed and therefore has a different snow accumulation regime than the other two sites. The upper and lower talus slopes are both overshadowed by cliff walls with average slopes of 65–70° and approximately 420 m of relief. The cliffs above the lower talus slope have a greater tendency for cornice formation than at the upper talus slope. Both measurement locations have a mean slope of 30–35° and face NNE. The validation slope was a safely accessible talus/failure slope in the interior of the watershed with no overhead relief. All locations, with the exception of the lowest part of the validation slope, exhibit rough topography with coarse, blocky surfaces.

2.3 Data collection and analysis methods

The laser was set-up at a stable platform using a bi-pod and the location was recorded using differential GPS (Sokkia GSR2700 ISX) which is accurate to 10 mm horizontally and 20 mm vertically. The location was marked for re-locating the laser for the snow-free survey; additionally, the coordinates were recorded with the differential GPS during both surveys. A deep snowpack (ca. 2 m) at the laser location necessitates that the laser is set up at the snow surface; therefore snow depth at the laser location is measured to aid in re-locating the laser for the snow-free survey. Accurate elevation data at the laser location is important to the success of the method, as all laser offsets are converted to Universal Transverse Mercator (UTM) coordinates and elevation relative to the laser location. The re-location of the laser was precise to within 3–8 cm horizontally and 12–17 cm vertically. The discrepancy in the vertical position of the laser result is a result of positioning the laser over snow during the spring survey.

Three locations were surveyed (Fig. 1) over two years: (1) upper talus slope (2008) (2) lower talus slope (2008 and 2009) and (3) validation slope (2009). During both years the lower talus slope was surveyed during peak accumulation (mid-April) whereas the upper talus slope was surveyed during the melt season (June) (Table 2). For each site, a second survey was conducted during September in snow-free conditions for each year. At the lower talus site a small amount of snow at the top of the slope did not melt and was present during the fall survey. At each location 187–1232 points were collected corresponding to a point density of 0.02–0.172 points per square metre (Table 2). The distance to the slope varied between 260–500 m.

Digital elevation surfaces were generated within the ESRI ArcGIS spatial computing software. Snow and snow-free digital elevation surfaces were created by spatially interpolating point data using a local polynomial interpolator. The two surfaces were then differenced to obtain an estimate of snow depth at the time of the initial survey.

2.4 Validation methods

Manual snow depth measurements were made at the validation slope on the same day as the laser survey. Snow depth data were collected using a centimetre graduated depth probe. Snow depth was measured at four points within a square metre to minimize the influence of local topographic variability and these values were subsequently averaged to obtain the snow depth at that point. A Trimble GeoXH handheld GPS was used to record the mid-point location of the manual snow depth measurement and these points were differentially post-corrected. Manually collected data points with greater than one metre of positional error were discarded. The manual snow depth measurement was compared to the nearest corresponding pixel in the calculated snow depth surface.

3 Results

3.1 Comparison of measured and calculated snow depths at the validation site

Snow depths from the two measurement methods (manual, laser) were compared at the validation slope to determine the accuracy of the laser method. The validation slope was surveyed with the laser on 20 April 2009, (Fig. 2a and b) and again in snow free conditions on 30 September 2009 (Fig. 2c). Snow depth was measured manually at 44 locations on 20 April 2009 following the acquisition of laser data (Fig. 2d). The center position of each of the 44 manual measurement locations was used to extract the corresponding calculated snow depth from the interpolated snow depth raster (Fig. 2d). In Fig. 3, the measured snow depth at each of the measurement locations is compared to calculated (laser) snow depth at the same location. The location number in Fig. 3 starts from upper left of the survey area (see Fig. 2d) and sequentially increases from the top to bottom, and left to right. The error bars represent the range in measured snow depth as determined by four measurements. Manually measured and calculated snow depths were in good agreement with a root-mean-square-error (RMSE) of 0.21 m or 12.3% of the average measured snow depth (Figs. 3 and 4). The spatial pattern (Fig. 3) of high and low snow depths is the same between the two methods.

A scatter plot of measured versus calculated snow depth (Fig. 4) illustrates the variability between the two measurement methods which can be attributed to several sources of error. Snow depth point measurements were not compared directly to laser measurements but rather to the interpolated surface (Fig. 2d) generated from the laser data. Therefore some of the scatter in Fig. 4 may be attributed to uncertainty inherent in using a statistical interpolation. There is additional uncertainty in the measured snow depth as it is impossible to quantify the true value of a continuously distributed medium with point measurements. However, despite the uncertainty associated with the snow depth at a given point, the spatial trends (Fig. 3) and the mean snow depths clearly indicate that the average snow depth distribution is well characterized. The average measured snow depth (Table 3) was 1.71 m and the calculated average was 1.70 m. Likewise, the measured (calculated) minimum of 0.73 m (0.79 m) and maximum of 2.43 m (2.45 m) indicate that the overall trend and features of the snow depth distribution are well captured using a laser distance device.

The snow depth distribution map (Fig. 2d) shows a large range in accumulated snow depths. Shallow snow on the west side (upper portion of the slope) is likely the result of a small cliff (approximately 5 m high) that shelters the slope immediately below (Fig. 2a and c) which is also indicated by exposed rocks at the base of the cliff. The remaining depth variation likely results from depressions in the surface topography which preferentially accumulate snow.

3.2 Talus slope snow accumulation patterns

There is a large range in snow depths on the talus slopes with much greater accumulation at the top of the slope versus the bottom (Figs. 5d, 6e and f). The upper talus slope has remaining snow accumulation in June of 1.15 m at the base of the slope and nearly 6 m at the top of the slope (Fig. 5d). The range in snow depths at the lower talus slope at the peak of the accumulation is even greater with a range of 2.76–7.59 m in 2008 and 1.73–8.92 m in 2009 (Fig. 6e and f).

The snow accumulation for the lower talus slope for 2008 and 2009 reveal a slightly different pattern between these two years. In 2008 there is a consistent transition from deep snow at the top of the slope to shallow snow at the bottom of the slope whereas in 2009 there is additional cross – slope variation. This is likely the result of a greater amount of snow redistribution by wind in 2009 than in 2008. In the winter of 2009 a greater proportion of high-wind events were from the southeast whereas the preceding three years of record indicate a dominant southwest winter flow regime. This change in wind direction would result in greater accumulation on the lee side of the slope which is indicated in the lower talus slope accumulation profile for 2009. In addition to the change in wind direction, average wind speeds were higher during 2009.

3.3 Contribution of spindrift and slough avalanches to snow accumulation

The change in snow depth along the length of the talus slopes was investigated by extracting snow accumulation profiles from the interpolated depth images (Figs. 5d, 6e and f). Extracted profiles (Fig. 7) show the change in snow depth with distance from the top of the talus slope to the bottom of the slope with the mean snow depth from all profiles in bold. These profiles indicate that deeper snow accumulation is located in a zone within 150 m of the cliff wall on the lower talus slope (Fig. 7a and b) and within 50 m of the cliff wall on the upper talus slope (Fig. 7c). The cliffs above the lower talus slope tend to focus snow accumulation as a result of converging slough avalanche paths which may be a possible explanation for the larger zone of influence at this site. Additionally, the cliffs at the lower cliff site have a tendency for cornice development that is not present at the upper talus site. Regardless, the accumulation profiles indicate that these regions are important hydrologically as the deep snow accumulation often persist into the late summer (Fig. 6b). Quantifying the zone of influence of the spindrift and slough avalanches will be useful in determining snow water equivalent in the watershed.

HESSD

7, 417–440, 2010

4 Conclusions

A laser rangefinder distance device was used to quantify snow depth on talus slopes in an alpine watershed. The device was used to determine distance to snow-covered slopes in the spring and again in the fall during snow-free conditions. The point data were then used to generate digital surface models of the snow covered and snow-free surfaces which can be used to determine snow depth by differencing of the two surfaces. Comparison of manually measured snow depths and snow depth calculated with the laser rangefinder indicate that this method is reliable with a RMS error of 0.21 m or 12.3% of the average snow depth. The spatial resolution of the laser rangefinder is coarser than similar technology such as terrestrial laser scanning; however, a laser rangefinder presents a more cost effective and portable means of measuring average snow depth in deep snow.

Snow depth distribution obtained using the laser rangefinder method shows that there is very deep snow accumulation at the top of talus slopes in the watershed as a result of slough and spindrift avalanching from the steep cirque walls overhead. This preferential accumulation is significant because these deep snow zones (ca. 6–9 m) persist into late August, effectively extending the snow melt season. Onset of snow melt earlier in the year and widespread glacial recession has raised concerns about a potential decline in late summer stream flow. Although late summer stream flow will likely be adversely affected by glacier retreat – it is important to quantify other sources of late summer hydrological inputs such as late lying snow that may potentially mitigate the loss of glacier melt water. At present, reliable methods of modeling or remotely measuring snow accumulation in very high relief alpine watersheds does not yet exist. This study has presented a simple method of measuring snow depth in complex alpine areas and contributes to an increased understanding of the hydrologic impact of snow redistribution by avalanches.

References

Allwardt, P. F., Bellahsen, N., and Pollard, D. D.: Curvature and fracturing based on global positioning system data collected at Sheep mountain anticline, Wyoming, Geosphere, 3, 408–421, 2007.

Barnett, T. P., Adam, J. C., and Lettenmaier, D. P.: Potential impacts of a warming climate on water availability in snow-dominated regions, 438, Nature, 438, 303–309, doi:10.1038/nature04141, 2005.

Deems, J. S., Fassnacht, S. R., and Elder, K. J.: Fractal distribution of snow depth from lidar data, J. Hydrometeorol., 7, 285–297, 2006.

Dozier, J. and Painter, T. H.: Multispectral and hyperspectral remote sensing of alpine snow properties, Annu. Rev. Earth Pl. Sc., 32, 465–494, 2004.

Elder, K., Dozier, J., and Michaelsen, J.: Snow accumulation and distribution in an alpine watershed, Water Resour. Res., 27, 1541–1552, 1991.

Fassnacht, S. R. and Deems, J. S.: Measurement sampling and scaling for deep montane snow depth data, Hydrol. Process., 20, 829–838, 2006.

Foster, J. L., Sun, C., Walker, J. P., Kelly, R., Chang, A., Dong, J., and Powell, H.: Quantifying the uncertainty in passive microwave snow water equivalent observations, Remote Sens. Environ., 94, 187–203, 2005.

Hamlet, A. F., Mote, P. W., Clark, M. P., and Lettenmaier, D. P.: Effects of temperature and precipitation variability on snowpack trends in the Western United States, J. Climate, 18, 4545–4561, 2005.

Hopkinson, C., Demuth, M. N., Sitar, M., and Chasmer, L. E.: Mapping the spatial distribution of snowpack depth beneath a variable forest canopy using airborne laser altimetry, 58th East. Snow Conf., Ottawa, Ontario, Canada, 2001, 249–253,

Ide, T. S., Pollard, D. D., and Orr Jr., F. M.: Fissure formation and subsurface subsidence in a coalbed fire, Int. J. Rock Mech. Min., 47(1), 81–93, 2009.

Lasercraft: Contour XLRic User's Manual, 2007.

Lewicki, J. L., Hilley, G. E., Tosha, T., Aoyagi, R., Yamamoto, K., and Benson, S. M.: Dynamic coupling of volcanic CO_2 flow and wind at the Horseshoe Lake tree kill, Mammoth mountain, California, Geophys. Res. Lett., 34, doi:10.1029/2006GL028848, 2007.

Lickorish, W. H. and Simony, P. S.: Evidence for late rifting of the Cordilleran margin outlined by stratigraphic division of the Lower Cambrian Gog group, Rocky Mountain main ranges,

British Columbia and Alberta, Can. J. Earth Sci., 32, 860–874, 1995.
Prokop, A.: Assessing the applicability of terrestrial laser scanning for spatial snow depth measurements, Cold Reg. Sci. Technol., 54, 155–163, 2008.
Prokop, A., Schirmer, M., Rub, M., Lehning, M., and Stocker, M.: A comparison of measurement methods: terrestrial laser scanning, tachymetry and snow probing for the determination of the spatial snow-depth distribution on slopes, Ann. Glaciol., 49, 210–216, 2008.
Rosenthal, W. and Dozier, J.: Automated mapping of montane snow cover at subpixel resolution from the Landsat thematic mapper, Water Resour. Res., 32, 115–130, 1996.
Schaffhauser, A., Adams, M., Fromm, R., Jorg P., Luzi, G., Noferini, L., and Sailer, R.: Remote sensing based retrieval of snow cover properties, Cold Reg. Sci. Technol., 54, 164–165, 2008.
St. Clair, C. C. and Forrest, A.: Impacts of vehicle traffic on the distribution and behaviour of rutting elk, *cervus elaphus*, Behavior, 146, 393–413, 2009.
Trujillo, E., Ramirez, J. A., and Elder, K. J.: Topographic, meteorologic, and canopy controls on the scaling characteristics of the spatial distribution of snow depth fields, Water Resour. Res., 43, doi:10.1029/2006WR005317, 2007.
Trujillo, E., Ramirez, J. A., and Elder, K. J.: Scaling properties and spatial organization of snow depth fields in sub-alpine forest and alpine tundra, Hydrol. Process., 23, 1575–1590, 2009.

HESSD
7, 417–440, 2010

Table 1. Laser specifications.

	Specifications for contour XLRic
Wavelength	905 nm at 200 Hz
Beam divergence	3 mR (equal to 0.5 m at distance of 500 m)
Range	Max: 1850, Min: 3 m
Accuracy	±0.1 m to a white target at 85 m
Acquire time	0.3 s
Inclination accuracy	±0.1 degree (equal to 0.9 m at distance of 500 m)
Bearing accuracy	±0.5 degree (equal to 4.3 m at distance of 500 m)
Operating temperature	−30 to +60 °C

HESSD

7, 417–440, 2010

Assessing the application of a laser rangefinder

J. L. Hood and M. Hayashi

Table 2. Laser data collection dates, number of data points, average distance to target and point density for four laser survey locations.

Location	Data collection	# of pts collected	Ave distance to target (m)	Point density (points/m^2)
Upper talus	20 Jun 08	500	380	0.134
	29 Sep 08	549		0.061
Lower talus	20 Apr 08	748	500	0.025
	30 Sep 08	1232		0.052
Lower talus	18 Apr 09	442	500	0.026
	30 Sep 09	408		0.023
Validation slope	18 Apr 09	187	260	0.103
	30 Sep 09	545		0.172

HESSD

7, 417–440, 2010

Assessing the application of a laser rangefinder

J. L. Hood and M. Hayashi

Table 3. Measured versus modeled mean, minimum, and maximum snow depth and standard deviation.

	Mean snow depth (m)	Minimum (m)	Maximum (m)	Standard deviation
Measured	1.71	0.73	2.43	0.40
Calculated	1.70	0.79	2.45	0.37

HESSD

7, 417–440, 2010

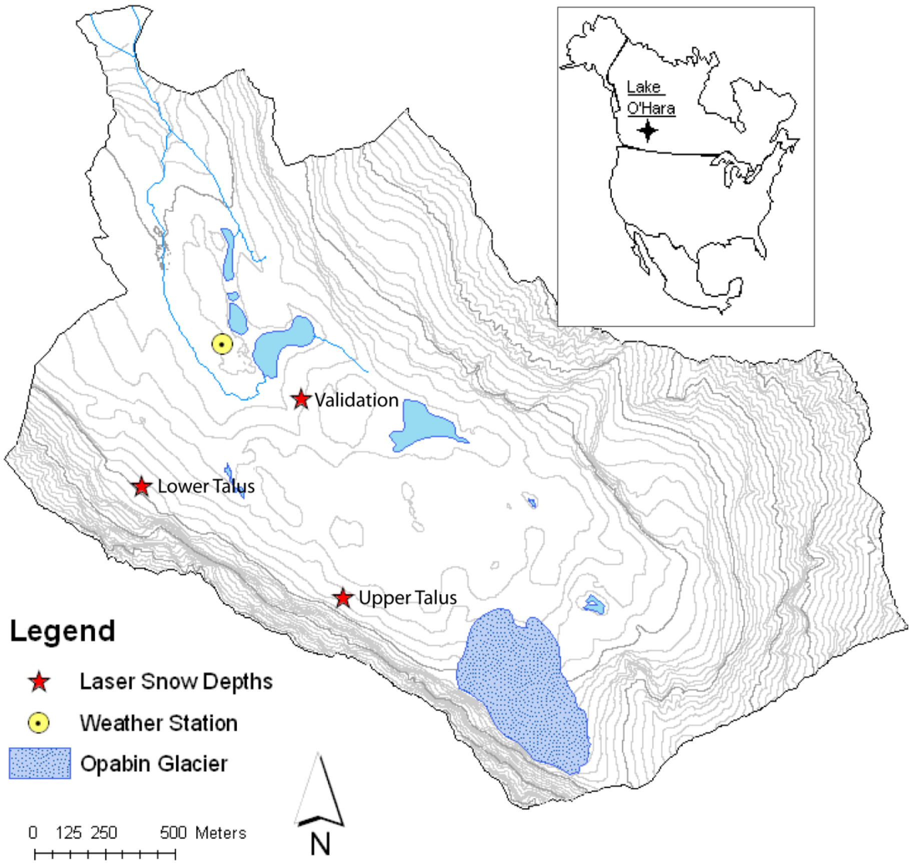

Fig. 1. Opabin watershed map with locations of laser surveys indicated. Contour interval 25 m.

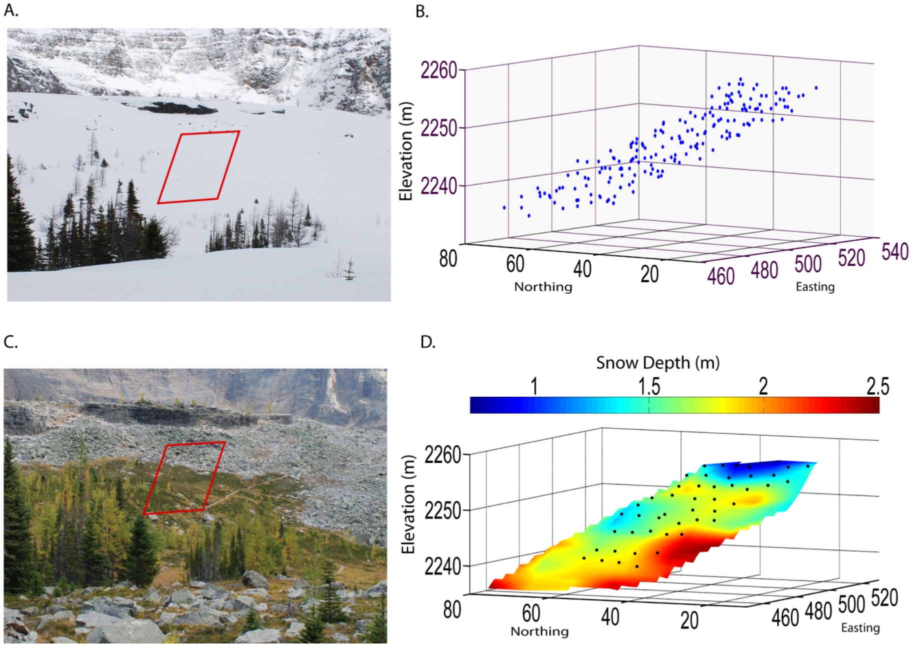

Fig. 2. Validation slope **(A)** Snow covered (18 April 2009) **(B)** Distribution of laser points (April) **(C)** Snow free (30 September 2009) **(D)** Calculated snow depth (black dots show locations of manual snow depth measurements).

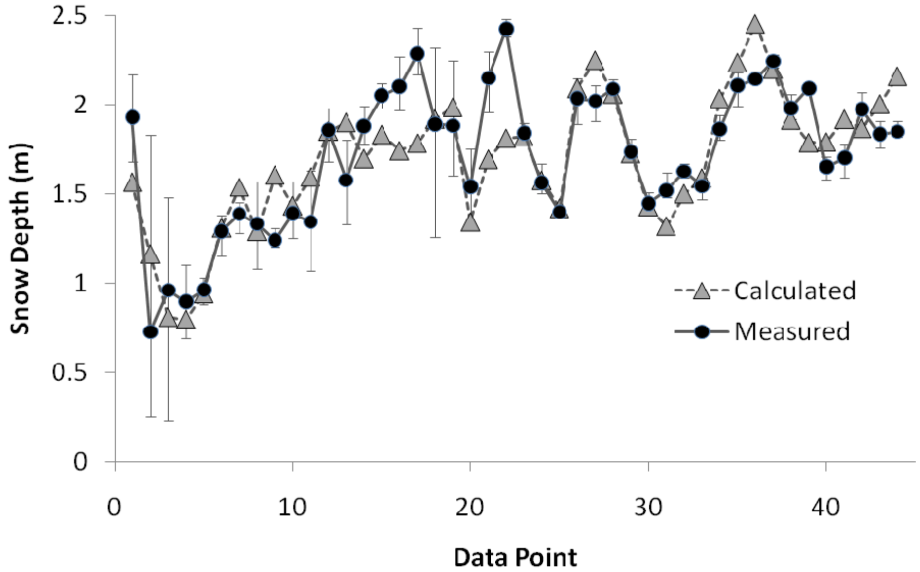

Fig. 3. Manually measured versus calculated snow depths at the validation slope.

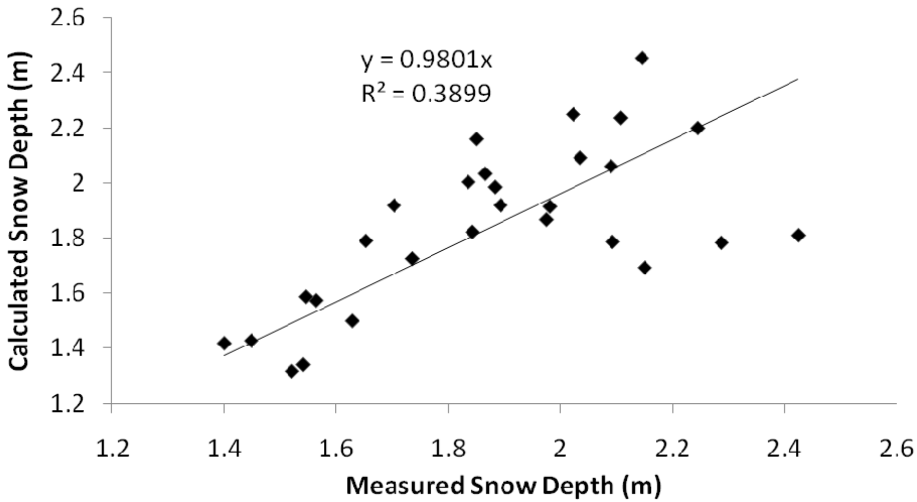

Fig. 4. Scatter plot of manually measured versus calculated snow depth at the validation slope.

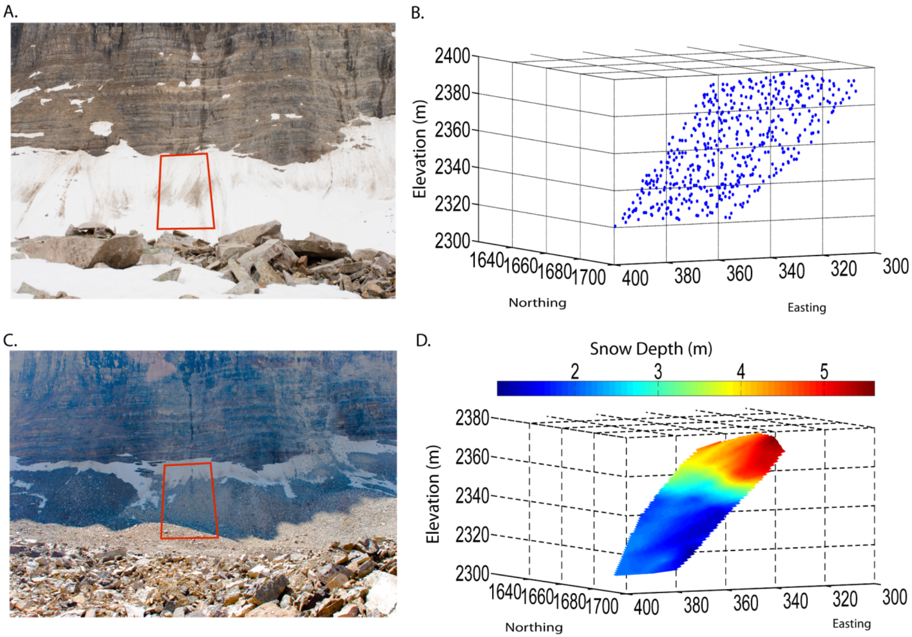

Fig. 5. Upper talus slope **(A)** Snow covered (20 June 2008) **(B)** Distribution of laser points (June) **(C)** Snow free (29 September 2008) **(D)** Calculated snow depth.

HESSD
7, 417–440, 2010

Assessing the application of a laser rangefinder

J. L. Hood and
M. Hayashi

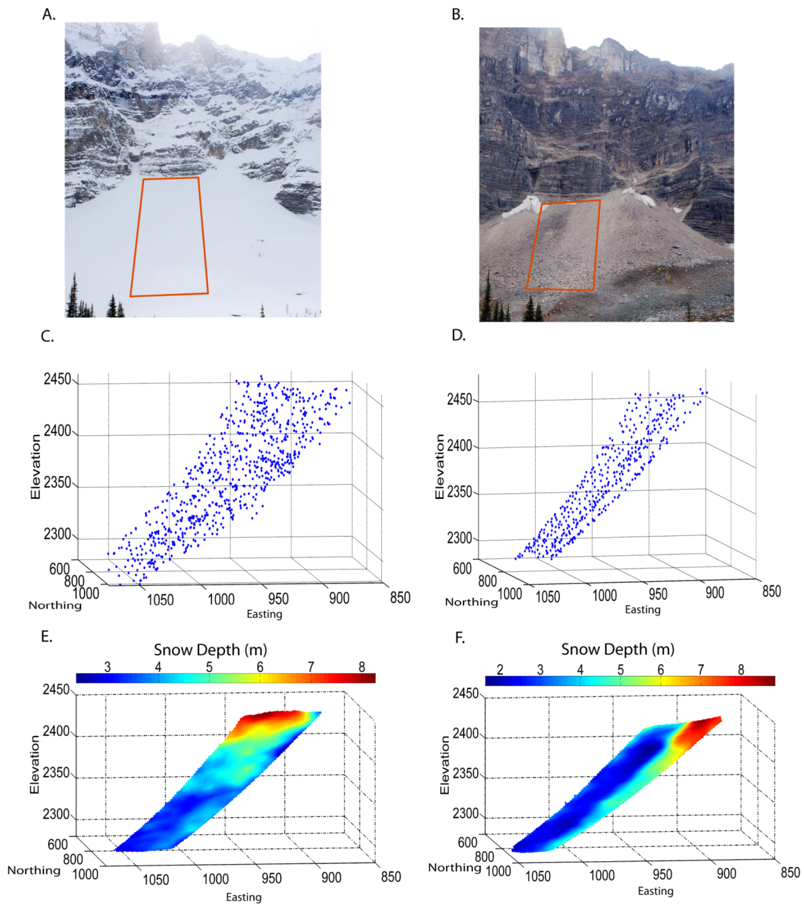

Fig. 6. Lower talus slope **(A)** Snow covered (28 April 2009) **(B)** Snow-free (30 September 2009) **(C)** Distribution of laser points (20 April 2008) **(D)** Distribution of laser points (18 April 2009) **(E)** Calculated snow depth (2008) **(F)** Calculated snow depth (2009).

HESSD

7, 417–440, 2010

Assessing the application of a laser rangefinder

J. L. Hood and M. Hayashi

Title Page
Abstract
Introduction
Conclusions
References
Tables
Figures
◀
▶
Back
Close
Full Screen / Esc
Printer-friendly Version
Interactive Discussion

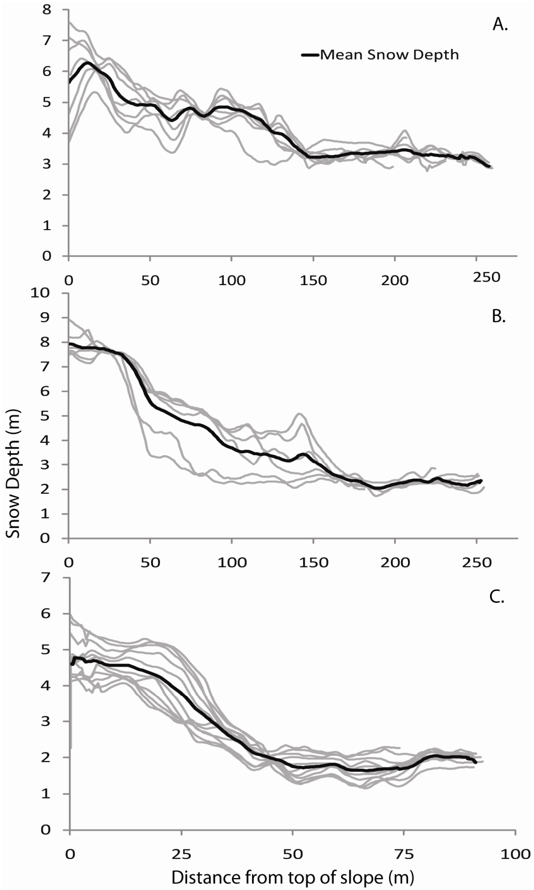

Fig. 7. Profiles of snow depth accumulation **(A)** Lower talus, 2008 **(B)** Lower talus, 2009 **(C)** Upper talus, 2008.

HESSD
7, 417–440, 2010